

12-1-2014

Astrophysical Tests of Kinematical Conformal Cosmology in Fourth-Order Conformal Weyl Gravity

Gabriele U. Variieschi

Loyola Marymount University, gvarieschi@lmu.edu

Repository Citation

Variieschi, Gabriele U., "Astrophysical Tests of Kinematical Conformal Cosmology in Fourth-Order Conformal Weyl Gravity" (2014). *Physics Faculty Works*. 14. http://digitalcommons.lmu.edu/phys_fac/14

Recommended Citation

Variieschi, G.U. Astrophysical Tests of Kinematical Conformal Cosmology in Fourth-Order Conformal Weyl Gravity. *Galaxies* **2014**, 2(4), 577-600. doi: [10.3390/galaxies2040577](https://doi.org/10.3390/galaxies2040577)

Article

Astrophysical Tests of Kinematical Conformal Cosmology in Fourth-Order Conformal Weyl Gravity

Gabriele U. Varieschi

Department of Physics, Loyola Marymount University, Los Angeles, CA 90045, USA;

E-Mail: gvarieschi@lmu.edu; Tel.: +1-310-338-7632; Fax: +1-310-338-5816

External Editor: Antonaldo Diaferio

Received: 16 October 2014; in revised form: 14 November 2014 / Accepted: 2 December 2014 /

Published: 12 December 2014

Abstract: In this work we analyze kinematical conformal cosmology (KCC), an alternative cosmological model based on conformal Weyl gravity (CG), and test it against current type Ia supernova (SNIa) luminosity data and other astrophysical observations. Expanding upon previous work on the subject, we revise the analysis of SNIa data, confirming that KCC can explain the evidence for an accelerating expansion of the Universe without using dark energy or other exotic components. We obtain an independent evaluation of the Hubble constant, $H_0 = 67.53 \text{ km s}^{-1} \text{ Mpc}^{-1}$, very close to the current best estimates. The main KCC and CG parameters are re-evaluated and their revised values are found to be close to previous estimates. We also show that available data for the Hubble parameter as a function of redshift can be fitted using KCC and that this model does not suffer from any apparent age problem. Overall, KCC remains a viable alternative cosmological model, worthy of further investigation.

Keywords: modified theories of gravity; conformal gravity; conformal cosmology; type Ia supernovae; standard candles; cosmic chronometers

PACS Classifications: 04.50.Kd; 04.50.-h; 98.80.-k

1. Introduction

Alternative theories of gravity (for reviews see [1,2]) have become more popular in recent years due to their ability to account for astrophysical observations without using dark matter (DM) and dark

energy (DE). However, the cosmological constant-cold dark matter model (Λ CDM) remains the standard explanation of current astrophysical knowledge [3].

Fourth-order conformal Weyl gravity (CG, for short, in the following) is the name given to an alternative gravitational theory, following the original work by Weyl [4], not to be confused with other theories based on conformal invariance. It was shown that CG [5,6] can describe the rotation curves of galaxies without DM [1,7–12] and can give rise to the accelerated expansion of the universe without resorting to DE [1,13].

A similar, but different approach to conformal cosmology was proposed by the current author in a series of papers [14–16] introducing a model which was called kinematical conformal cosmology [14] (KCC in the following) since it was based on purely kinematic considerations, without using any dynamical equation of state for the Universe. This model was able to account for the accelerated expansion of the Universe [15] and might also be able to explain the origin of some gravitational anomalies, such as the Pioneer Anomaly [16] and the Flyby Anomaly [17].

Both models, the “standard” CG cosmology by Mannheim and KCC, were critically analyzed by Diaferio *et al.* [18] and compared to standard Λ CDM cosmology by applying a Bayesian approach to available astrophysical data from type Ia supernovae (SNIa) and gamma-ray bursts. Contrary to the authors’ expectations [18], the results of this analysis showed that Λ CDM, Mannheim’s CG, and KCC can all describe the current astrophysical data equally well. Therefore, models based on conformal gravity can be considered viable alternatives to Λ CDM and are worthy of further investigation.

In addition, a recent study by Yang *et al.* [19] has tested Mannheim’s CG against recent astrophysical data from SNIa, determinations of the Hubble parameter at different redshift, and in relation to the “age problem” of the old quasar APM 08279+5255 at $z = 3.91$. The outcome of this analysis is that CG can describe all these astrophysical data in a satisfactory manner and does not suffer from an age problem, as opposed to the case of Λ CDM.

Following this recent work, the goal of this paper is to test our KCC against the same astrophysical data used in Reference [19] in order to ascertain whether KCC is still a viable cosmological model. In Section 2, we begin by reviewing the main results of conformal gravity and KCC. In Section 3, the main part of our paper, we will constrain the KCC parameters, by using the latest Union 2.1 SNIa data, and show that KCC can produce Hubble plots of the same quality as those obtained with standard Λ CDM. In Section 4, we will compare the experimental data for the Hubble parameter, as a function of redshift z , with KCC predictions and also briefly analyze the age problem in the context of KCC.

2. Conformal Gravity and Kinematical Conformal Cosmology

Conformal Gravity is based on the Weyl action:

$$I_W = -\alpha_g \int d^4x (-g)^{1/2} C_{\lambda\mu\nu\kappa} C^{\lambda\mu\nu\kappa}, \quad (1)$$

where $g \equiv \det(g_{\mu\nu})$, $C_{\lambda\mu\nu\kappa}$ is the conformal or Weyl tensor, and α_g is a dimensionless coupling constant. I_W is the unique general coordinate scalar action that is invariant under local conformal transformations: $g_{\mu\nu}(x) \rightarrow e^{2\alpha(x)} g_{\mu\nu}(x) = \Omega^2(x) g_{\mu\nu}(x)$. CG does not suffer from the cosmological

constant problem and is renormalizable [20]; it is a ghost-free theory [21,22], although it still faces some theoretical challenges ([23–28]).

The fourth-order CG field equations, $4\alpha_g W_{\mu\nu} = T_{\mu\nu}$ (where $W_{\mu\nu}$ is the Bach tensor—see [1,14] for full details), were studied in 1984 by Riegert [29], who obtained the most general, spherically symmetric, static electrovacuum solution. The explicit form of this solution, for the practical case of a static, spherically symmetric source in CG, *i.e.*, the fourth-order analogue of the Schwarzschild exterior solution in General Relativity (GR), was then derived by Mannheim and Kazanas in 1989 [5,6]. This latter solution, in the case $T_{\mu\nu} = 0$ (exterior solution), is described by the metric

$$ds^2 = -B(r) c^2 dt^2 + \frac{dr^2}{B(r)} + r^2(d\theta^2 + \sin^2 \theta d\phi^2), \quad (2)$$

with

$$B(r) = 1 - 3\beta\gamma - \frac{\beta(2 - 3\beta\gamma)}{r} + \gamma r - \kappa r^2. \quad (3)$$

The three integration constants in the last equation are as follows: β (cm) can be considered the CG equivalent of the geometrized mass $\frac{GM}{c^2}$, where M is the mass of the (spherically symmetric) source and G is the universal gravitational constant; two additional parameters, γ (cm^{-1}) and κ (cm^{-2}), are required by CG, while the standard Schwarzschild solution is recovered for $\gamma, \kappa \rightarrow 0$ in the equations above. The quadratic term $-\kappa r^2$ indicates a background De Sitter spacetime, which is important only over cosmological distances, since κ has a very small value. Similarly, γ measures the departure from the Schwarzschild metric at smaller distances, since the γr term becomes significant over galactic distance scales.

The values of the CG parameters were first determined by Mannheim [1] (Other estimates of these parameters exist in the literature. For example, in Reference [30], constraints on the value of the γ constant were obtained by studying the perihelion shift of planetary motion in CG.):

$$\gamma = 3.06 \times 10^{-30} \text{ cm}^{-1}, \quad \kappa = 9.54 \times 10^{-54} \text{ cm}^{-2}. \quad (4)$$

In our previous KCC publications [14,15] we have shown a different way to compute the CG parameters, obtaining values which differ by a few orders of magnitude from those above:

$$\gamma = 1.94 \times 10^{-28} \text{ cm}^{-1}, \quad \kappa = 6.42 \times 10^{-48} \text{ cm}^{-2}. \quad (5)$$

We will revise and update the values of these parameters in Section 3 by constraining them with recent astrophysical data.

Mannheim *et al.* ([1,7–12]) used the CG solutions in Equations (2) and (3) to perform extensive data fitting of galactic rotation curves without any DM contribution, with the values of γ and κ as in Equation (4). Although the values of these CG parameters are very small, the linear and quadratic terms in Equation (3) become significant over galactic and/or cosmological distances.

This also means that CG solutions (including those for other types of sources, see discussion in [17]) are not asymptotically flat, thus raising the question of possible “gravitational redshift” effects at large distances. In fact, this was the main motivation for our “kinematical approach” to conformal cosmology: in regions far away from massive sources (for $r \gg \beta(2 - 3\beta\gamma)$) and also ignoring the term $\beta\gamma$, as suggested by the analysis of galactic rotation velocities, $B(r)$ simplifies to

$$B(r) = 1 + \gamma r - \kappa r^2. \quad (6)$$

This implies a possible gravitational redshift at large distances, analogous to the one experimentally observed in standard GR near massive sources such as the Earth, the Sun, or white dwarfs. This effect is related to the square-root of the ratio of the time-time components g_{00} of the metric at two different locations. In Reference [14] we considered our current spacetime location ($r = 0; t_0$) in relation to the spacetime location ($r > 0; t < t_0$) of a distant galaxy which emits light at a time t in the past that reaches us at present time t_0 and appears to be redshifted in relation to the standard redshift parameter z .

We then argued that this observed redshift could be due (in part, or totally) to the gravitational redshift effect mentioned above. If this effect were indeed the only source of the observed redshift, with the metric in Equation (6), we would have:

$$1 + z = \sqrt{\frac{-g_{00}(0, t_0)}{-g_{00}(r, t)}} = \frac{1}{\sqrt{1 + \gamma r - \kappa r^2}}. \quad (7)$$

In other words, if the CG metric in Equations (2) and (3) has a true physical meaning, as it seems to be the case from the detailed fitting of galactic rotational curves, it should also determine strong gravitational redshift at very large cosmological distances. (Equation (6) is valid for regions far away from massive sources, *i.e.*, for $r \gg \beta(2 - 3\beta\gamma) \simeq 2\beta \simeq 2\frac{GM}{c^2}$, where M can be considered the mass of the largest structures in our Universe, such as galaxies, or clusters of galaxies. Therefore, the resulting characteristic distance r represents the scale at which our kinematical approach is appropriate. For example, considering the estimated mass of a cluster, or a supercluster of galaxies, the resulting characteristic distance is approximately $r \gtrsim 0.1 - 10 \text{ Mpc}$, which shows that KCC mainly applies to the inter-galactic or cosmological scale.) As far as we are aware, this issue has never been raised in all current CG literature (except, of course, in our previous papers).

The CG metric in Equations (2) and (6) is actually conformal to the standard FRW metric (see details in [5] or [14]):

$$ds^2 = -c^2 dt^2 + \mathbf{a}^2(\mathbf{t}) \left[\frac{d\mathbf{r}^2}{1 - \mathbf{k}\mathbf{r}^2} + \mathbf{r}^2(d\theta^2 + \sin^2\theta d\phi^2) \right], \quad (8)$$

where $\mathbf{a}(\mathbf{t})$ is the standard Robertson-Walker scale factor, $\mathbf{k} = k/|k| = 0, \pm 1$ and $k = -\gamma^2/4 - \kappa$. As in our previous papers, we distinguish here between two sets of coordinates: the Static Standard Coordinates-SSC (r, t) used in Equations (2), (3), (6) and (7), as opposed to the FRW coordinates (\mathbf{r}, \mathbf{t})—in bold—used in Equation (8) (Similarly, bold type characters will be used for quantities referring to the FRW geometry, while normal type characters will be used with reference to the SSC coordinates. For example, the RW scale factor will be denoted here as $\mathbf{a}(\mathbf{t})$ or $a(t)$, respectively, in the two cases. In our previous papers we used $\mathbf{R}(\mathbf{t})$ and $R(t)$ for the scale factor, but we now prefer to adopt the more common notation, $\mathbf{a}(\mathbf{t})$ or $a(t)$, in this work). Full details of the complete transformations between these coordinates can be found in our References [14,15].

This local conformal invariance induces a dependence of the length and time units on the local metric, so that the observed redshift can be interpreted as the ratio between the wavelength $\lambda(\mathbf{r}, \mathbf{t})$ of the radiation emitted by atomic transitions, at the time and location of the source, and the wavelength $\lambda(\mathbf{0}, \mathbf{t}_0)$ of the same atomic transition measured here on Earth at current time. Since modern metrology defines our common units of length δl and time δt as being proportional respectively to the wavelength and to the

period (inverse of the frequency ν) of radiation emitted during certain atomic transitions, we can write the following “redshift equation”

$$1 + z = \frac{\mathbf{a}(\mathbf{t}_0)}{\mathbf{a}(\mathbf{t})} = \frac{\lambda(\mathbf{r}, \mathbf{t})}{\lambda(\mathbf{0}, \mathbf{t}_0)} = \frac{\delta l(\mathbf{r}, \mathbf{t})}{\delta l(\mathbf{0}, \mathbf{t}_0)} = \frac{\nu(\mathbf{0}, \mathbf{t}_0)}{\nu(\mathbf{r}, \mathbf{t})} = \frac{\delta t(\mathbf{r}, \mathbf{t})}{\delta t(\mathbf{0}, \mathbf{t}_0)}, \quad (9)$$

connecting wavelengths λ to unit-lengths δl and frequencies ν to unit-time intervals δt (we also use $\lambda\nu = c$, with a constant speed of light c).

Therefore, in KCC the observed redshift is due to the change of length and time units over cosmological spacetime, as opposed to the standard explanation of a pure expansion of the scale factor \mathbf{a} . In view of this interpretation, and connecting together Equations (7) and (9), KCC is able to derive directly the scale factor as a function of space or time coordinates, without solving the dynamical field equations. In terms of SSC, we have:

$$1 + z = \frac{a(0)}{a(r)} = \frac{1}{\sqrt{1 + \gamma r - \kappa r^2}}, \quad (10)$$

or, using appropriate coordinate transformations, in terms of FRW coordinates:

$$1 + z = \frac{\mathbf{a}(\mathbf{0})}{\mathbf{a}(\mathbf{r})} = \sqrt{1 - \mathbf{k} \mathbf{r}^2} - \delta \mathbf{r}, \quad (11)$$

with

$$\delta = \frac{\gamma}{2} \begin{cases} |k|^{-1/2} & \text{for } k \neq 0 \\ 1 & \text{for } k = 0 \end{cases}. \quad (12)$$

All these scale-factor equations can also be written explicitly in terms of the time coordinates t and \mathbf{t} , as is usually done in standard cosmology, by computing the time it takes for a light signal, emitted at radial distance r or \mathbf{r} , to reach the observer at the origin. The detailed expressions for $a(t)$ and $\mathbf{a}(\mathbf{t})$, as well as all the connecting formulas between the different variables and conformal parameters, can be found in Reference [14] (see Table 1). Furthermore, from the plots of the KCC scale factors, such as $\mathbf{a}(\mathbf{r})$ from Equation (11), it can be seen that the observed redshift $z > 0$ is only possible for $\mathbf{k} = -1$, so that the other two cases, $\mathbf{k} = 0, +1$, are actually ruled out.

The new CG dimensionless parameter $\delta = \frac{\gamma}{2\sqrt{|k|}}$ (for $\mathbf{k} = -1$) in Equation (12) becomes the most important quantity in KCC (The parameter δ in Equation (12) is dimensionless only for $\mathbf{k} = \pm 1$. For the $\mathbf{k} = 0$ case, Equation (11) simply becomes $1 + z = \mathbf{a}(\mathbf{0})/\mathbf{a}(\mathbf{r}) = 1 - \frac{\gamma}{2}\mathbf{r}$. In this particular case, the coordinate \mathbf{r} has dimensions of length, so this equation is still dimensionally correct (in this case the scale factor $\mathbf{a}(\mathbf{t})$ becomes a dimensionless quantity, so that Equation (8) is also correct). This is due to the particular form of the transformation between SSC and FRW coordinates, for the special $k = 0$ case. See Section 3.1 in Reference [14] for complete details.): it combines together the original CG parameters γ and κ , in view also of the relation between k and κ

$$k = -\frac{\gamma^2}{4} - \kappa \quad (13)$$

already mentioned above. (In our previous papers, we considered the possibility that all these CG parameters might also be changing with spacetime coordinates. In particular, we supposed that the δ

parameter might play the role of a universal time and we used the zero subscript to denote the current values of all these parameters (*i.e.*, δ_0 , γ_0 , *etc.*). In this paper, we are just considering the current values of these parameters, so we simply write δ , γ , κ , *etc.*) It can be shown that $|\delta| < 1$ and that, for $k = -1$, Equation (11) yields the following direct relation between r and z :

$$\mathbf{r} = \frac{\delta(1+z) \pm \sqrt{(1+z)^2 - (1-\delta^2)}}{1-\delta^2}. \quad (14)$$

The plus-minus sign in the last equation indicates that there are two locations where $z = 0$: at the origin $\mathbf{r} = 0$, and at a particular radial location $\mathbf{r}_{rs} = \frac{2\delta}{1-\delta^2}$ which becomes of physical significance for $\delta > 0$. In fact, in this particular case, there is a region of negative redshift (*i.e.*, a blueshift) for $0 < \mathbf{r} < \mathbf{r}_{rs}$, followed by a standard redshift region at larger radial distances, for $\mathbf{r} > \mathbf{r}_{rs} = \frac{2\delta}{1-\delta^2}$. This suggests that the (current) value of δ should be small and positive, so that the supposed blueshift region would be a small (practically undetectable) region around the observer: for example, a small region of the size of the Solar System, or similar.

In two of our previous papers [15,16] we actually suggested that this local blueshift region could have been the origin of the Pioneer Anomaly (PA—for a review, see [31]) since “blueshifted” signals coming from the Pioneer spacecraft would appear to be equivalent to the observed anomalous acceleration. In view of this possible connection, the value of the γ parameter in Equation (5) was directly inferred from the Pioneer anomalous acceleration [15,16]; the value of the δ parameter was then computed [15] from the fitting of the SNIa data available at the time, and the values of the parameters k and κ were obtained through Equations (12) and (13). In summary, the values of the CG parameters were determined as follows (see also Table 1 in Reference [15]):

$$\delta = 3.83 \times 10^{-5}, \quad \gamma = 1.94 \times 10^{-28} \text{ cm}^{-1}, \quad k = -6.42 \times 10^{-48} \text{ cm}^{-2}, \quad \kappa = 6.42 \times 10^{-48} \text{ cm}^{-2}. \quad (15)$$

Although it is still possible that the PA might have a gravitational origin, *i.e.*, due to modifications of GR, it is now widely accepted that the cause of this anomaly is probably more mundane [32]: thermal recoil forces originating from the spacecraft radioactive thermoelectric generators. Therefore, in the following sections we will perform a new computation of the CG parameters in Equation (15), without using any more data related to the PA. We will begin, in the following section, by constraining our parameters using updated SNIa data.

3. KCC and Type Ia Supernovae

In order to constrain the CG parameters with recent SNIa data we need to redefine the luminosity distance in KCC, since this is the main cosmological distance used in this context. In this section we will expand upon concepts already introduced in Reference [15] (more details about the definitions of distances in KCC can be found in this reference). We start by noticing that the new interpretation of the redshift discussed in the previous section (in particular, in Equation (9)) implies that lengths and time intervals scale with redshift z as:

$$\begin{aligned} \Delta l_z &= (1+z) \Delta l_0 \\ \Delta t_z &= (1+z) \Delta t_0, \end{aligned} \quad (16)$$

where the subscript 0 indicates intervals of the given quantity associated with objects which share the same spacetime location of the observer at the origin (namely, here on Earth at $r = 0$ and at our current time t_0), while the subscript z indicates intervals of the same quantity associated with objects at redshift $z \neq 0$, as seen or measured by the same observer at the origin.

It should be emphasized that this change in lengths, or time intervals (as well as wavelengths, frequencies, and all other kinematical quantities derived from lengths and times), is due to the spacetime location of the object being studied (as measured by the redshift parameter z) and not to the “cosmic expansion” as in the standard cosmological model.

It is natural to assume that masses, energies, luminosities, and other dynamical quantities will follow similar scaling laws, but not necessarily the same as the one in Equation (16). In Reference [15] we assumed the following scaling laws for masses and energies (Mass and energy will scale in the same way, since $\Delta E \propto \Delta l^2 \Delta t^{-2} \Delta m$, with lengths and times scaling in the same manner, due to Equation (16)):

$$\begin{aligned}\Delta m_z &= f(1+z) \Delta m_0 \\ \Delta E_z &= f(1+z) \Delta E_0,\end{aligned}\tag{17}$$

where $f(1+z)$ is some arbitrary function of $(1+z)$, so that $\lim_{z \rightarrow 0} f(1+z) = 1$.

As a consequence of these scaling laws, the “absolute luminosity” L , or energy emitted per unit time, will scale as

$$L_z = \frac{f(1+z)}{(1+z)} L_0,\tag{18}$$

where the meaning of the subscripts is the same as described above for the other quantities. Thus, KCC postulates a change in the absolute luminosity of a “standard candle”, which is intrinsically due to its spacetime location, while standard cosmology assumes an invariable absolute luminosity L of the standard candle being considered.

Standard cosmology defines the luminosity distance as $d_L = \sqrt{\frac{L}{4\pi l}} = \mathbf{a}_0 \mathbf{r} (1+z)$, with L and l being the absolute and apparent luminosities of the standard candle being used as a distance indicator; \mathbf{a}_0 denotes the current value of the scale factor and the $(1+z)$ factor on the right-hand side of the equation originates from a $(1+z)^2$ dimming factor under the square root. This factor is due to the standard redshift of the photon frequency and also to a time dilation effect of the emission interval of photons.

KCC considers instead this $(1+z)^2$ dimming factor as unphysical, so the $(1+z)$ factor on the right-hand side of the standard luminosity distance equation is completely eliminated. In view also of our scaling law for luminosities in Equation (18), and of Equation (14), we then define the luminosity distance in KCC as (In the following equation we choose the positive sign in front of the square root to select the solution corresponding to past redshift, $z > 0$ for $\mathbf{r} > \mathbf{r}_{rs} = 2\delta/(1-\delta^2)$, which is the correct choice for the following analysis of SNIa data)

$$d_L \equiv \sqrt{\frac{L_z}{4\pi l}} = \sqrt{\frac{f(1+z) L_0}{(1+z) 4\pi l}} = \mathbf{a}_0 \mathbf{r} = \mathbf{a}_0 \frac{\delta(1+z) + \sqrt{(1+z)^2 - (1-\delta^2)}}{(1-\delta^2)}.\tag{19}$$

Since this definition assumes an intrinsic dimming of the luminosity L_z with redshift z , it leads to distance estimates which are dramatically different from those of standard cosmology for different values of z (see the first three columns in Table 2 of Reference [15]).

To avoid this issue, an alternative definition could be employed, which would retain the concept of an invariable luminosity L_0 of a standard candle, while including the other aspects of KCC. We can obtain this alternative luminosity distance \tilde{d}_L by modifying the previous equation as follows:

$$\tilde{d}_L \equiv \sqrt{\frac{L_0}{4\pi l}} = \sqrt{\frac{(1+z)}{f(1+z)}} \mathbf{a}_0 \mathbf{r} = \sqrt{\frac{(1+z)}{f(1+z)}} \mathbf{a}_0 \frac{\delta(1+z) + \sqrt{(1+z)^2 - (1-\delta^2)}}{(1-\delta^2)}, \quad (20)$$

so that the right-hand side of the equation now depends explicitly on the still unknown function $f(1+z)$. In Table 2 of Reference [15], it was shown that distances estimated using \tilde{d}_L are very close to those of standard cosmology (compare the values in the fourth column of this table with those in the third or fifth columns), so the KCC definition in Equation (20) more closely agrees with the luminosity distance of standard cosmology.

We will see in the following that both definitions, in Equations (19) and (20), lead to the same results when applied to SNIa data, but they differ conceptually: the former assumes a variable absolute luminosity L_z of a standard candle, while the latter assumes an invariable absolute luminosity L_0 , which is more in line with the standard interpretation.

Before we can apply these definitions to the analysis of SNIa data, we need to obtain an explicit form for the $f(1+z)$ function, which enters most of the KCC equations above. Expanding upon the arguments discussed in our previous work [15], we can assume the following properties for this function:

- (1) f is some arbitrary function of $(1+z)$, with a “fixed point” at 1, that is, $f(1) = 1$, or $\lim_{z \rightarrow 0} f(1+z) = 1$.
- (2) f is a dimensionless quantity, so that Equations (17)–(20) are dimensionally correct.
- (3) f is a function possibly built out of other expressions of KCC, which also depend on the factor $(1+z)$.

Although the last property in the list above is just an educated guess, it suggests that the function f might depend on the following KCC factor:

$$\frac{d_L}{d_{REF}} = \frac{\delta(1+z) + \sqrt{(1+z)^2 - (1-\delta^2)}}{2\delta}, \quad (21)$$

constructed as the (dimensionless) ratio between the luminosity distance in Equation (19) and the reference distance

$$d_{REF} = \mathbf{a}_0 \mathbf{r}_{rs} = \mathbf{a}_0 \frac{2\delta}{1-\delta^2}, \quad (22)$$

which corresponds to the value \mathbf{r}_{rs} of the radial coordinate (other than the origin) where we have $z = 0$ (see discussion after Equation (14)). Therefore, as it was argued also in Reference [15], d_{REF} represents the ideal reference distance at which we should place a “standard candle” of given absolute luminosity L_0 : at this location its luminosity is not affected by the scaling effect of Equation (18), since $z = 0$ for $\mathbf{r} = \mathbf{r}_{rs}$. In KCC d_{REF} is the equivalent of the standard reference distance of 10 parsec, used for standard candles, such as supernovae.

Following the discussion above, the most general form of the function $f(1+z)$ that we will consider is:

$$f(1+z) = \frac{(1+z)^\beta}{\left(\frac{d_L}{d_{REF}}\right)^\alpha} = \left[\frac{2\delta}{\delta(1+z) + \sqrt{(1+z)^2 - (1-\delta^2)}} \right]^\alpha (1+z)^\beta, \quad (23)$$

where α and β are coefficients to be determined from SNIa data fitting. Again, the choice of the function $f(1+z)$ in the previous equation is just an educated guess, an “ansatz” based on the only two functions of $(1+z)$ introduced in KCC: a function $(1+z)^\beta$, which generalizes the simple $(1+z)$ scaling factor in Equation (16), and a function $1/(d_L/d_{REF})^\alpha$, which generalizes the inverse-square dependence of the apparent luminosity of a radiation source upon the (luminosity) distance between the observer and the source.

3.1. SNIa Data Fitting

In our previous work, we determined the CG parameters by using the SNIa data available at the time (292 SNIa data of the “gold-silver” set, see [15] for details) and by considering the value of the Pioneer anomalous acceleration. As already mentioned, we will not use the PA data in this study, but we will use the latest compilation of SNIa data: the 580 supernovae from the Union 2.1 data set ([33–35]).

The distance modulus μ (difference between the apparent magnitude m and the absolute magnitude M) is usually computed, using Pogson’s law, in terms of the logarithm of the ratio between the apparent luminosity l_z (at redshift z) and the reference apparent luminosity l_{REF} (at the reference distance of choice). It can then be expressed in terms of absolute luminosities and distances, using the general relation $l = \frac{L}{4\pi d_L^2}$. We have:

$$\mu(z) = m(z) - M = -2.5 \log_{10} \left(\frac{l_z}{l_{REF}} \right) = -2.5 \log_{10} \left(\frac{L_z}{L_{REF}} \frac{d_{REF}^2}{d_L^2} \right), \quad (24)$$

where the subscript z refers to quantities evaluated at redshift $z \neq 0$, while the subscript REF indicates the “reference” value of the quantity, *i.e.*, when the standard candle is placed at the reference distance.

As explained before, we have two possible choices for this reference distance: the traditional distance of 10 pc (since usually the absolute luminosity L of a “standard candle” is defined as the apparent luminosity of the same object placed at 10 parsec) and the KCC reference distance d_{REF} in Equation (22) above, since this is the only location, other than the origin, where $z = 0$.

Using this latter choice for the reference distance and combining Equation (24) with Equations (18), (19), (21) and (23), we obtain explicitly:

$$\begin{aligned} \mu(z) &= 2.5(2 + \alpha) \log_{10}(d_L/d_{REF}) + 2.5(1 - \beta) \log_{10}(1 + z) \\ &= 2.5(2 + \alpha) \log_{10} \left[\frac{\delta(1+z) + \sqrt{(1+z)^2 - (1-\delta^2)}}{2\delta} \right] + 2.5(1 - \beta) \log_{10}(1 + z), \end{aligned} \quad (25)$$

an expression which can be used directly to fit SNIa data and determine the value of the three free parameters α , β , and δ .

Using this last equation as a fitting formula for the Union 2.1 SNIa data, we obtained the following “best-fit” values for the free parameters:

$$\alpha = 2.096 \pm 0.027, \quad \beta = 1.141 \pm 0.091, \quad \delta = (4.120 \pm 0.221) \times 10^{-5}. \quad (26)$$

Assuming that α and β are likely to be integer numbers, due to their role in the definition of the function $f(1+z)$ in Equation (23), and close to the values reported in the previous equation, we repeated the fitting procedure, first by setting $\beta = 1$:

$$\alpha = 2.058 \pm 0.010, \beta = 1, \delta = (3.817 \pm 0.087) \times 10^{-5}, \quad (27)$$

then by fixing both α and β as follows:

$$\alpha = 2, \beta = 1, \delta = (3.356 \pm 0.005) \times 10^{-5}. \quad (28)$$

All these fits have good statistical quality ($R^2 = 0.996$) and clearly confirm the results of our past SNIa data fitting [15], where it was a priori postulated that $\alpha = 2$, $\beta = 1$, and δ was found to be as in Equation (15). It can also be shown that our fitting formula in the second line of Equation (25) can even be obtained by using the alternative definition of the luminosity distance \tilde{d}_L in Equation (20), with appropriate changes in all formulas leading to Equation (25). Thus, our SNIa data fitting procedure is valid even if we use \tilde{d}_L instead of d_L , which is equivalent to using a luminosity distance whose estimates are very close to those of standard cosmology.

In KCC, the values of the CG parameters γ and δ are also connected to the current value of the Hubble parameter:

$$\begin{aligned} H_0 &= \frac{\gamma}{2}c \\ \mathbf{H}_0 &= \frac{c}{\mathbf{a}_0}\delta \end{aligned} \quad (29)$$

in SSC or FRW coordinates, respectively, but with $H_0 \simeq \mathbf{H}_0$ for $|\delta| \ll 1$ [15]. Since in this work we are not relying any longer on the PA data, we can now derive the value of γ directly from the Hubble constant, using the previous equation.

The Union 2.1 SNIa data are consistent with the Hubble constant estimate by Riess *et al.* [36], $H_0 = (73.8 \pm 2.4) \text{ km s}^{-1} \text{ Mpc}^{-1}$, from which we obtain $\gamma = \frac{2}{c}H_0 = (1.596 \pm 0.052) \times 10^{-28} \text{ cm}^{-1}$. However, the most commonly used estimate of the Hubble constant is from the Planck collaboration 2013 results [37]:

$$H_0 = (67.3 \pm 1.2) \text{ km s}^{-1} \text{ Mpc}^{-1} \implies \gamma = \frac{2}{c}H_0 = (1.455 \pm 0.026) \times 10^{-28} \text{ cm}^{-1}; \quad (30)$$

therefore, in the rest of this paper we will consider the value of γ above as the current KCC estimate.

It could be argued that, since the Union 2.1 SNIa data are based on the standard definitions for the luminosity distance, standard candles, *etc.*, it might be more appropriate to use $d_{REF} = 10 \text{ pc}$ as a reference distance. This leads to a slightly different fitting formula, in view also of Equations (19) and (29):

$$\begin{aligned} \mu(z) &= 2.5(2 + \alpha) \log_{10}(d_L/d_{REF}) + 2.5(1 - \beta) \log_{10}(1 + z) \\ &= 2.5(2 + \alpha) \left\{ \log_{10} \left[\delta \frac{\delta(1+z) + \sqrt{(1+z)^2 - (1-\delta^2)}}{h(1-\delta^2)} \right] + 8.4768 \right\} \\ &\quad + 2.5(1 - \beta) \log_{10}(1 + z), \end{aligned} \quad (31)$$

which also includes the “normalized Hubble constant” h as a fitting parameter. This dimensionless quantity is related to H_0 as follows:

$$H_0 = 100 h \text{ km s}^{-1} \text{ Mpc}^{-1} = 3.2408 \times 10^{-18} h \text{ s}^{-1}. \quad (32)$$

As in our previous fitting Formula (25), we now have the option of leaving all four parameters (α , β , δ , and h) completely free, or to fix some of them, for example, by choosing integer values for α and β . If we leave all four parameters free, our best fit to Union 2.1 SNIa data yields:

$$\alpha = 2.005 \pm 0.253, \beta = 0.766 \pm 0.421, \delta = 3.45 \times 10^{-5}, h = 0.71, \quad (33)$$

in line with our previous estimate of the parameters in Equation (26) and with our preferred value for H_0 in Equation (30). If we fix the value of the Hubble constant as in Equation (30), *i.e.*, $h = 0.673$, and also set $\alpha = 2$, $\beta = 1$, as it was done in Equation (28), we obtain instead:

$$\alpha = 2, \beta = 1, \delta = (3.367 \pm 0.008) \times 10^{-5}, h = 0.673. \quad (34)$$

Comparing our results for δ , in Equations (28) and (34), we see that our two possible fitting Formulas (25) and (31) produce consistent results for $\delta \simeq 3.36 - 3.37 \times 10^{-5}$, in line also with our previous determinations from Reference [15], or in Equation (15). In addition, our analysis confirms that the $f(1+z)$ function in Equation (23) should be considered with $\alpha = 2$ and $\beta = 1$, *i.e.*,

$$f(1+z) = \frac{1+z}{\left(\frac{d_L}{d_{REF}}\right)^2} = \left[\frac{2\delta}{\delta(1+z) + \sqrt{(1+z)^2 - (1-\delta^2)}} \right]^2 (1+z). \quad (35)$$

Although our two fitting formulas, Equations (25) and (31), both yield similar results, we have to choose one of the two methods for a final determination of the CG parameters. Since the former fitting formula assumes $d_{REF} = a_0 \frac{2\delta}{1-\delta^2}$, which is more consistent with the KCC model, while the latter formula assumes $d_{REF} = 10 \text{ pc}$, which is more consistent with standard cosmology, our final choice will be the first expression (as it was also done previously in Equation (43) of Reference [15]).

Therefore, in view of Equations (12), (13), (28), and (30) our revised set of KCC parameters is the following:

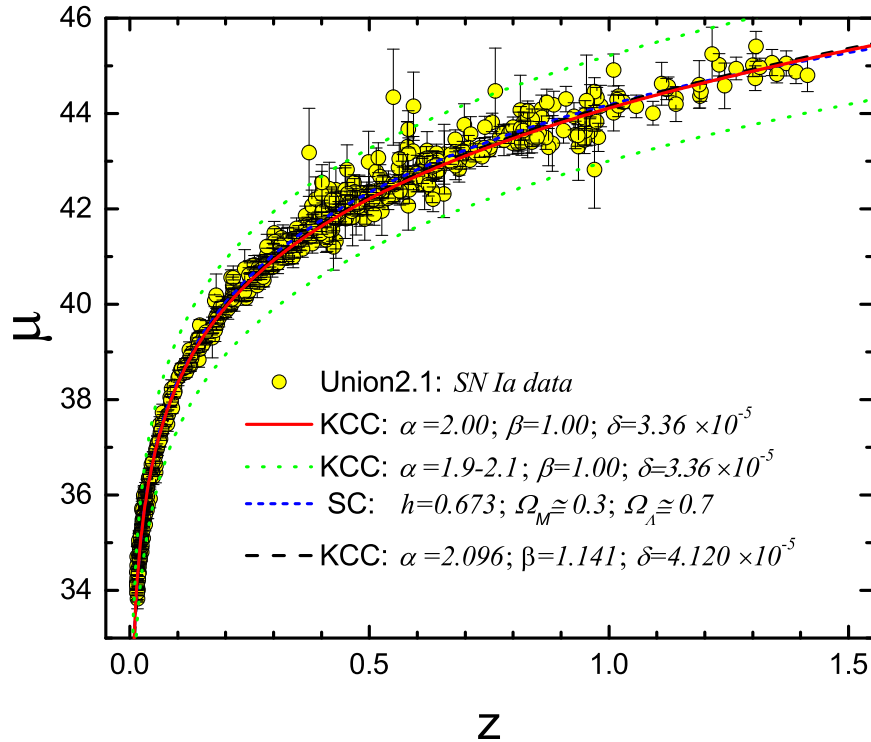
$$\delta = 3.36 \times 10^{-5}, \gamma = 1.46 \times 10^{-28} \text{ cm}^{-1}, k = -4.70 \times 10^{-48} \text{ cm}^{-2}, \kappa = 4.70 \times 10^{-48} \text{ cm}^{-2}, \quad (36)$$

and the function $f(1+z)$ is given in Equation (35). In the next section we will plot our results and compare them with those of standard cosmology.

3.2. Union 2.1 Data and KCC Plots

As already mentioned at the beginning of Section 3.1, our new KCC fits were performed with the latest Union 2.1 SNIa data (Also available in electronic form at: <http://supernova.lbl.gov/Union/>) ([33–35]). The Supernova Cosmology Project “Union2.1” SNIa compilation is an update of the previous “Union2” compilation, bringing together data for 833 supernovae, drawn from 19 datasets. Of these, 580 SNe pass usability cuts and are included in the data set. In Figure 1 we plot these 580 data points (distance modulus μ vs. redshift z) together with the standard cosmology (SC) Hubble plot (blue, short-dashed curve), obtained with standard values of the critical densities ($\Omega_M \cong 0.3$, $\Omega_\Lambda \cong 0.7$) and with the Hubble constant value in Equation (30), *i.e.*, $h = 0.673$.

Figure 1. Data from Union 2.1 SNIa set [35] are fitted with Equation (25). Our KCC fits (red-solid for fixed α and β ; black long-dashed for variable α and β) show very good statistical quality ($R^2 = 0.996$) and are very close to the standard cosmology prediction (SC, blue short-dashed). Also shown (dotted-green curves) is the range of our KCC fitting curves for a variable $\alpha = 1.9 - 2.1$.



Our KCC fits are also presented in this figure: in red, solid curve, we show our main fit, using Equation (25) and with the values of the parameters as in Equation (28); the green-dotted curves show how our fits depend on changes of the α parameter (in the range $\alpha = 1.9 - 2.1$), keeping the other parameters unchanged. Finally, the black, long-dashed curve is our KCC fit with the parameters as in Equation (26), *i.e.*, when all the parameters are left free in the fitting procedure. This curve is practically the same as our main KCC fit in solid-red, and both KCC curves are very close to the standard cosmology theoretical prediction.

In Figure 2 we reproduce the same data and the same fitting curves as in Figure 1, but in the form of a standard Hubble plot, with logarithmic axis for redshift z . In this way, all the fitting curves become almost straight lines and the differences between them can be better appreciated. Again, the two main KCC fits (red-solid and black-long dashed) are almost indistinguishable and only slightly different from the equivalent standard cosmology prediction (blue, short-dashed).

Similarly, Figure 3 presents the same information in the form of residual values $\Delta\mu$, with the baseline represented by our main KCC fit (red-solid, with parameters as in Equation (28)). In this figure it is easier to notice the small differences between our two KCC fits and the standard cosmology prediction. It is also evident that most of the SNIa data points fall within the $\alpha = 1.9 - 2.1$ band.

Figure 2. The same data and fitting curves presented in Figure 1 are shown here in a standard Hubble plot, with logarithmic axis for the redshift z . The meaning of the symbols and of the different plots is the same as in the previous figure.

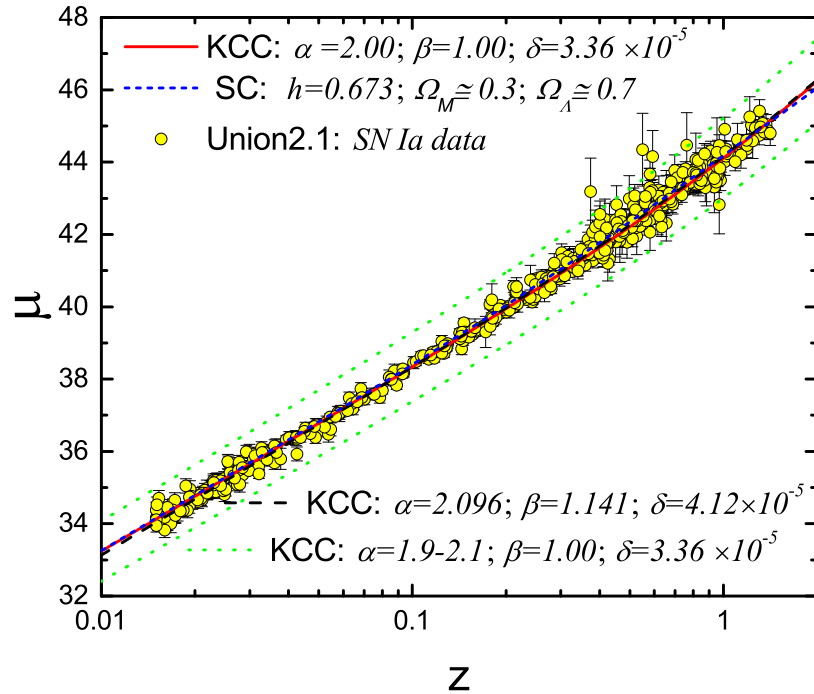
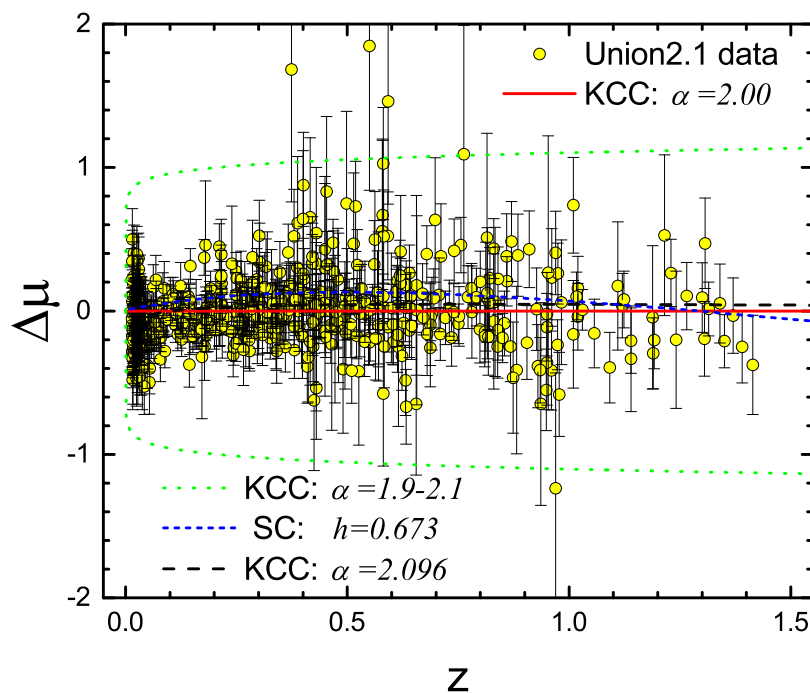


Figure 3. Data from Union 2.1 SNIa set [35] are fitted with Equation (25) and shown as residuals $\Delta\mu$. The baseline is represented by our main KCC fit (red-solid curve, with parameters as in Equation (28)). The meaning of the other curves and symbols is the same as in the previous figures.



The last study we performed, in connection with the Union 2.1 data, was related to the low- z behavior of our fitting formulas. As already discussed at length in [15], we cannot effectively expand in powers of z our luminosity distance d_L in Equation (19), due to the very small value of the δ parameter. Therefore, we just discard terms containing δ in the same expression for d_L and retain only the leading term depending on z :

$$d_L \simeq a_0 \sqrt{2z}. \quad (37)$$

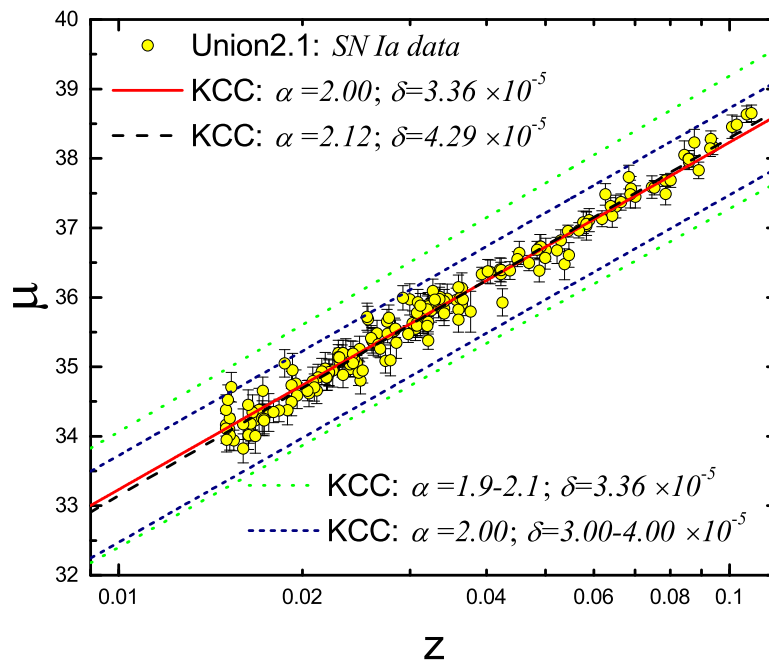
Using this expression and $d_{REF} \simeq a_0 2\delta$, from Equation (22), in Equation (25) and also assuming $\beta = 1$, as suggested by previous fits, we have:

$$\mu(z) = 2.5(2 + \alpha) \log_{10}(d_L/d_{REF}) \simeq 2.5(2 + \alpha) \log_{10} \left(\frac{\sqrt{2z}}{2\delta} \right), \quad (38)$$

which becomes our “low- z ” fitting formula.

To check this expression we selected 179 SNIa data from the Union 2.1 set with $z \lesssim 0.1$ and applied our fitting Formula (38) to this data subset. Figure 4 shows the results of this low- z fitting: our main KCC fit (red-solid curve), for a fixed $\alpha = 2$, yields $\delta = (3.359 \pm 0.001) \times 10^{-5}$, essentially the same result as in Equation (28) for the whole set of 580 supernovae. Leaving both parameters free (black, long-dashed curve) yields instead $\alpha = 2.121 \pm 0.040$, $\delta = (4.287 \pm 0.340) \times 10^{-5}$, and the two KCC curves almost coincide. In this figure we also show how our low- z fit is sensitive to the value of α in the range 1.9 – 2.1 (green-dotted curves) and to the value of δ in the range $(3.00 - 4.00) \times 10^{-5}$ (blue, short-dashed curves).

Figure 4. A subset of Union 2.1 SNIa data [35], for $z \lesssim 0.1$, is fitted with Equation (38). Our low- z KCC fits (red-solid curves for fixed α ; black long-dashed curves for variable α) yield essentially the same results as in the previous fits, which used the full range of values for z . Also shown are the ranges of our KCC fitting curves, for a variable $\alpha = 1.9 - 2.1$ (green-dotted curves) and for a variable $\delta = (3.00 - 4.00) \times 10^{-5}$ (blue, short-dashed curves).



In our previous work (see Section 3.2 in [15]) we also remarked that our low- z distance modulus expression in Equation (38), for $\alpha = 2$, can be rewritten as $\mu(z) \simeq 10 \log_{10} \left(\frac{\sqrt{2z}}{2\delta} \right) = 5 \log_{10} \left(\frac{z}{2\delta^2} \right)$, so that it corresponds perfectly to the first terms of the standard cosmology expansion $\mu(z) \simeq 25 + 5 \log_{10} \left(\frac{cz}{H_0} \right) = 5 \log_{10} \left(10^5 \frac{cz}{H_0} \right)$, neglecting higher-order terms in z . Comparing the right-hand sides of these two “low- z ” expressions, we find a direct connection between the Hubble constant and the KCC δ parameter:

$$\mathbf{H}_0 \simeq H_0 = 2 \times 10^5 c \delta^2 = 67.53 \text{ km s}^{-1} \text{ Mpc}^{-1}, \quad (39)$$

having used our best estimate for δ in Equation (28) and with the speed of light given as $c = 299792.458 \text{ km s}^{-1}$.

It is very remarkable that our KCC model and the related SNIa data fitting are able to obtain an estimate for the Hubble constant which is very close to the 2013 Planck collaboration value. We want to emphasize that our value for δ in Equation (28) came from the fitting formula in Equation (25), which is independent of any assumed value for \mathbf{H}_0 .

Therefore, our value of \mathbf{H}_0 in Equation (39) represents KCC’s direct evaluation of the Hubble constant, in agreement with current best estimates. We can recompute the value for γ using $H_0 = 67.53 \text{ km s}^{-1} \text{ Mpc}^{-1}$ as $\gamma = \frac{2}{c} H_0 = 1.460 \times 10^{-28} \text{ cm}^{-1}$, which is essentially equivalent to our previous estimate in Equation (30), based on the 2013 Planck collaboration value for \mathbf{H}_0 . Following these two estimates, our final value for γ will be quoted as $\gamma \simeq 1.46 \times 10^{-28} \text{ cm}^{-1}$, as already reported in Equation (36).

4. KCC and Hubble Parameter Data

Another important test of our KCC model can be performed in relation with observed data for the Hubble parameter $H(z)$, measured as a function of redshift. As it was done by Yang *et al.* in their recent analysis [19] of Mannheim’s CG, we will use here all the available data for $H(z)$, obtained from different sources and with different methods, as reported in Table 1 (When both statistical and systematic errors were quoted (as in [38,39]), we summed these errors in quadrature and reported the total error in the table).

Although different methods were used to obtain the data in this table, the most common argument relies on the fact that the Hubble parameter depends on the differential age of the Universe, as a function of redshift, in the form:

$$\mathbf{H}(z) = -\frac{1}{1+z} \frac{dz}{dt}. \quad (40)$$

Therefore, a determination of $\frac{dz}{dt}$, or more practically of the ratio $\frac{\Delta z}{\Delta t}$ between finite intervals of redshift and time, will lead to a direct measurement of $\mathbf{H}(z)$.

In order to measure the time interval Δt , we need to identify and use so-called “cosmic chronometers”, *i.e.*, astrophysical objects, such as galaxies, whose evolution follows a known fiducial model, so that these objects behave as “standard clocks” in the Universe.

Table 1. Available Hubble parameter data $H(z)$, from various sources, obtained with different methods.

z	$H(z)$ (km s ⁻¹ Mpc ⁻¹)	Source	Method (See Text)
0.0900	69 ± 12	Jimenez <i>et al.</i> (2003) [40]	DA
0.1700	83 ± 8	Simon <i>et al.</i> (2005) [41]	DA
0.2700	77 ± 14	Simon <i>et al.</i> (2005) [41]	DA
0.4000	95 ± 17	Simon <i>et al.</i> (2005) [41]	DA
0.9000	117 ± 23	Simon <i>et al.</i> (2005) [41]	DA
1.3000	168 ± 17	Simon <i>et al.</i> (2005) [41]	DA
1.4300	177 ± 18	Simon <i>et al.</i> (2005) [41]	DA
1.5300	140 ± 14	Simon <i>et al.</i> (2005) [41]	DA
1.7500	202 ± 40	Simon <i>et al.</i> (2005) [41]	DA
0.4800	97 ± 62	Stern <i>et al.</i> (2010) [42]	DA
0.8800	90 ± 40	Stern <i>et al.</i> (2010) [42]	DA
0.1791	75 ± 4	Moresco <i>et al.</i> (2012) [38]	DA
0.1993	75 ± 5	Moresco <i>et al.</i> (2012) [38]	DA
0.3519	83 ± 14	Moresco <i>et al.</i> (2012) [38]	DA
0.5929	104 ± 13	Moresco <i>et al.</i> (2012) [38]	DA
0.6797	92 ± 8	Moresco <i>et al.</i> (2012) [38]	DA
0.7812	105 ± 12	Moresco <i>et al.</i> (2012) [38]	DA
0.8754	125 ± 17	Moresco <i>et al.</i> (2012) [38]	DA
1.0370	154 ± 20	Moresco <i>et al.</i> (2012) [38]	DA
0.2400	79.69 ± 2.65	Gaztañaga <i>et al.</i> (2009) [39]	BAO
0.4300	86.45 ± 3.68	Gaztañaga <i>et al.</i> (2009) [39]	BAO
0.0700	69 ± 19.6	Zhang <i>et al.</i> (2012) [43]	DA
0.1200	68.6 ± 26.2	Zhang <i>et al.</i> (2012) [43]	DA
0.2000	72.9 ± 29.6	Zhang <i>et al.</i> (2012) [43]	DA
0.2800	88.8 ± 36.6	Zhang <i>et al.</i> (2012) [43]	DA
0.4400	82.6 ± 7.8	Blake <i>et al.</i> (2012) [44]	BAO and GC
0.6000	87.9 ± 6.1	Blake <i>et al.</i> (2012) [44]	BAO and GC
0.7300	97.3 ± 7.0	Blake <i>et al.</i> (2012) [44]	BAO and GC
0.3500	82.1 ± 5	Chuang <i>et al.</i> (2012) [45]	GC

Once this population of standard clocks has been found and dated, the “differential-age” technique can be used: the age difference Δt , and the corresponding redshift difference Δz , between two of these cosmic chronometers can be measured, thus determining $H(z)$ in view of Equation (40). This differential age (DA) method has the advantage of not using any integrated cosmological quantity (such as the luminosity distance, which is expressed through an integral in standard cosmology), since these quantities depend on the integral of the expansion history, thus yielding less direct measurements of the expansion history itself.

Since the original proposal of this DA method [40,46], the best choice of “cosmic chronometers” was found to be a population of “red-envelope” galaxies: massive galaxies, harbored in high-density regions

of galaxy clusters and containing the oldest stellar populations, which are now evolving only passively (*i.e.*, with very limited new star formation). The age of these passively evolving galaxies can then be used in connection with the DA technique explained above to measure $\mathbf{H}(z)$ [40–42]. A similar approach, also based on passively evolving galaxies, but more centered on a differential spectroscopic evolution of early-type galaxies as a function of redshift, was introduced by Moresco *et al.* [38,47], yielding more data points, followed by the more recent work by Zhang *et al.* [43].

A different approach [39] to the measurement of $\mathbf{H}(z)$ considered instead the baryon acoustic oscillations (BAO) peak position as a standard ruler in the radial direction. This BAO method was later connected to the Alcock-Paczynski distortion from galaxy clustering (GC) in the WiggleZ Dark Energy Survey [44], and one additional data point was recently obtained [45] by using galaxy clustering data. All the measured data points for $\mathbf{H}(z)$ are reported in Table 1; we will now interpret these data in view of our kinematical conformal cosmology.

In KCC, the Hubble parameter is directly related to z as follows (see Equation (10) in [15]):

$$\mathbf{H}(z) = \frac{c}{a_0} \sqrt{(1+z)^2 - (1-\delta^2)} = \frac{\mathbf{H}_0}{\delta} \sqrt{(1+z)^2 - (1-\delta^2)}, \quad (41)$$

in view also of Equation (29) and assuming $\delta > 0$. At first, it seems impossible to fit the observational Hubble data (OHD) in Table 1 with the formula on the right-hand side of the last equation, for $\delta \sim 10^{-5}$ and \mathbf{H}_0 close to standard values. However, the OHD are obtained essentially from Equation (40), or rather from the critical determination of the time interval $\Delta t \approx dt$, which enters the denominator on the right-hand side of this equation.

Although the differential age methods used to obtain these OHD in the literature are slightly different (and even more different are the methods based on BAO and/or GC), they all rely heavily on time, distance, and spectroscopic determinations, based on standard cosmology. Since KCC allows for intrinsic scaling of lengths, time intervals, energies, luminosities, etc., as in Equations (16) and (18), we need to allow the presence of these scaling factors, such as powers of $(1+z)$ and/or $f(1+z)$, into our fitting Formula (41).

In view also of the general form of $f(1+z)$ in Equation (23), we generalize our fitting formula for $\mathbf{H}(z)$ as:

$$\begin{aligned} \mathbf{H}(z) &= \frac{\mathbf{H}_0}{\delta} \frac{(1+z)^l}{\left(\frac{d_L}{d_{REF}}\right)^m} \sqrt{(1+z)^2 - (1-\delta^2)} \\ &= 2 \times 10^5 c \delta (1+z)^l \left[\frac{2\delta}{\delta(1+z) + \sqrt{(1+z)^2 - (1-\delta^2)}} \right]^m \sqrt{(1+z)^2 - (1-\delta^2)}, \end{aligned} \quad (42)$$

where l and m are free parameters to be determined with our fitting procedure. The additional factor of $(1+z)^l / (d_L/d_{REF})^m$, introduced in the last equation, is justified in the same way as it was done in Equation (23): it is just a reasonable “ansatz” based on the only two functions of $(1+z)$ introduced in KCC. Of course, the new parameters l and m in Equation (42) are not necessarily related to the similar α and β parameters used before with the SNIa data, since we are now fitting a different type of astrophysical data. In the last equation we also used our direct connection in Equation (39) between \mathbf{H}_0 and δ to avoid over-parametrizing this fitting formula.

We then used our revised Formula (42) to fit the OHD in Table 1, allowing up to three dimensionless parameters: δ , l , and m . However, leaving all three parameters completely free does not lead to a satisfactory fit of the data, so we simply set δ to our preferred value: $\delta = 3.36 \times 10^{-5}$. Our best fit, considering l and m as free parameters, is:

$$l = 1.288 \pm 0.084, m = 1.092 \pm 0.006, \delta = 3.36 \times 10^{-5}, \quad (43)$$

and is shown in Figure 5 (red-solid curve), together with all the OHD from Table 1. If we fix l to be an integer value, close to the previous estimate, we obtain instead:

$$l = 1, m = 1.075 \pm 0.003, \delta = 3.36 \times 10^{-5}, \quad (44)$$

which is also shown in Figure 5 (black, long-dashed curve). In the same figure, the standard cosmology prediction, $\mathbf{H}(z) = \mathbf{H}_0 \sqrt{\Omega_M(1+z)^3 + \Omega_\Lambda + \Omega_R(1+z)^4 + \Omega_K(1+z)^2}$, is shown (blue, short-dashed curve) for $\Omega_M \cong 0.3$, $\Omega_\Lambda \cong 0.7$, $\Omega_R = \Omega_K \approx 0$, and $\mathbf{H}_0 = 67.3 \text{ km s}^{-1} \text{ Mpc}^{-1}$.

The $l \simeq 1$ value for the first parameter in our KCC fitting formula can be explained as originating from the scaling law of time intervals, $\Delta t_z = (1+z) \Delta t_0$, applied to the measured value $\Delta t \approx dt$ which enters Equation (40). In other words, the observed age differences at redshift z are actually Δt_z intervals, but the age intervals entering Equation (40) should be considered as Δt_0 intervals, since standard cosmology does not allow for rescaled quantities. Thus, combining Equations (40) and (41), we have: $\mathbf{H}(z) = -\frac{1}{1+z} \frac{\Delta z}{\Delta t_0} = (1+z) \frac{\mathbf{H}_0}{\delta} \sqrt{(1+z)^2 - (1-\delta^2)}$, where the $(1+z)$ factor on the right-hand side is due to the rescaling of the time intervals.

Figure 5. OHD from Table 2 are fitted with our KCC Equation (42), using values for the parameters as in Equation (43) (red-solid curve), or as in Equation (44) (black, long-dashed curve). Also shown is the standard cosmology prediction (blue, short-dashed curve).

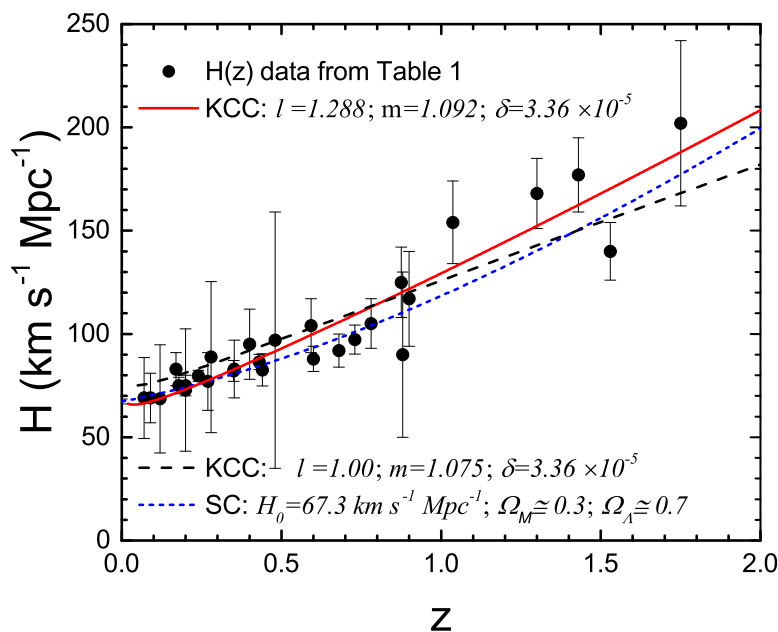


Table 2. Standard Cosmology and KCC estimates for the age of the Universe and of quasar APM 08279+5255.

Model	Age of Universe	Age of Quasar
SC ($\Omega_M \cong 0.3, \Omega_\Lambda \cong 0.7, \mathbf{H}_0 = 67.3 \text{ km s}^{-1} \text{ Mpc}^{-1}$)	14.0 Gyr	1.34 Gyr
KCC—parameters from Equation (43)	14.2 Gyr	1.65 Gyr
KCC—parameters from Equation (44)	15.8 Gyr	2.45 Gyr

The $m \approx 1$ value for the second parameter in our KCC fits is not so easily explained. This corresponds to a factor $1/\left(\frac{d_L}{d_{REF}}\right)^m$ on the right-hand side of our fitting Formula (42), with m close to unity. This could be due to the fact that the OHD are determined through spectroscopic measurements (involving the scaling factor $f(1+z) = (1+z)/(d_L/d_{REF})^2$), or because the age determinations of the cosmic chronometers, such as the “red-envelope” galaxies, involve their luminosity distances, thus allowing for the KCC correction factor (d_L/d_{REF}) to appear in our fitting formula.

In particular, age estimates are typically sensitive to the distance scale (see discussion in Reference [48], pp. 62–63): a fractional change $\delta d/d$ in distance estimates will produce a change $\delta L/L = -2\delta d/d$ in absolute luminosities and thus a fractional change $\delta t/t \approx +2\delta d/d$ in age estimates, since the absolute luminosity of stars at the turn-off point in the main sequence is roughly inversely proportional to the age of the globular cluster being studied. In KCC the change in luminosity distance δd_L is due to the difference between the revised $d_L = \sqrt{\frac{f(1+z)}{(1+z)} \frac{L_0}{4\pi l}}$ of Equation (19) and the standard cosmology expression $d_L = \sqrt{\frac{L_0}{4\pi l}}$, which assumes an invariable luminosity L_0 .

Therefore, in view also of Equation (35), a fractional change $\delta d_L/d_L = \sqrt{\frac{f(1+z)}{(1+z)}} - 1 = 1/\left(\frac{d_L}{d_{REF}}\right) - 1$ might introduce a correcting factor $1 + \delta d_L/d_L = 1/\left(\frac{d_L}{d_{REF}}\right)$ into our CG age estimates and ultimately yield a corresponding factor $1/\left(\frac{d_L}{d_{REF}}\right)^m$ on the right-hand side of our fitting Formula (42), with $m \approx 1$. Due to the complexity of the details related to the experimental measurements of the OHD, at this point we are unable to further explain the presence of this factor in our fitting formula for $\mathbf{H}(z)$.

Finally, we wish to comment on the “age problem” analyzed in Reference [19], which was related to Mannheim’s CG. The issue being studied was a possible age problem for the old quasar APM 08279+5255 at $z = 3.91$, as well as the current estimates of the age of the Universe. As already remarked in Section 1, it was shown that CG does not suffer from an age problem, as it might be the case instead for standard cosmology (see again [19] and references therein).

For a cosmological model where $\mathbf{H}(z)$ is known explicitly, all age estimates are essentially obtained by integrating Equation (40). For instance, the current age of the Universe t_0 is:

$$t_0 = T(0, \infty) = - \int_{\infty}^0 \frac{1}{(1+z) \mathbf{H}(z)} dz, \quad (45)$$

assuming $z = \infty$ at time zero and $z = 0$ at current time. More generally, the age of an astrophysical object (such as the old quasar mentioned above) which is observed at redshift z , but whose formation occurred at earlier times, corresponding to a formation redshift $z_f > z$, is computed as:

$$T(z, z_f) = - \int_{z_f}^z \frac{1}{(1+z)\mathbf{H}(z)} dz. \quad (46)$$

In Λ CDM cosmology, using the standard expression for $\mathbf{H}(z)$ with $\Omega_M \cong 0.3$, $\Omega_\Lambda \cong 0.7$, $\Omega_R = \Omega_K \approx 0$, and $\mathbf{H}_0 = 67.3 \text{ km s}^{-1} \text{ Mpc}^{-1}$, the age of the Universe from Equation (45) is computed as $t_0 = 14.0 \text{ Gyr}$, in line with estimates based on globular clusters, or other astrophysical objects. On the contrary, the quasar APM 08279+5255 is observed at $z = 3.91$, with an estimated formation redshift $z_f = 15$ [19]. Using Equation (46), the standard cosmology age for this quasar would be $T_{SC}(3.91, 15) = 1.34 \text{ Gyr}$, causing a possible age problem, since the best estimated age for this quasar is 2.1 Gyr , with a 1σ lower limit of 1.8 Gyr and an absolute lowest limit of 1.5 Gyr [19].

As discussed at length in our previous work (see Section 4.5 in Reference [14]), in KCC we have two possible time coordinates: the static standard coordinate t related to our local unit of time, as opposed to the FRW coordinate \mathbf{t} , where the former is essentially the conformal time of the latter. When using the former coordinate t , the Universe does not appear to have initial or final singularities (thus, the age of the Universe would be infinite, if measured using this coordinate), while both singularities appear when using the latter coordinate \mathbf{t} .

However, if we use FRW coordinates to estimate ages, *i.e.*, if we use $\mathbf{H}(z)$ as in Equations (41), (45) and (46), we would obtain extremely small estimates for the age of the Universe and for the age of the quasar being studied. This shows that age estimates in KCC are not directly comparable with age estimates in SC, in the same way that luminosity distances in KCC and SC are widely different, as already mentioned in Section 3.

Once again, to reconcile the two different views, we must use the “revised” formula for $\mathbf{H}(z)$ in Equation (42) with the KCC parameters determined in Equation (43), or Equation (44). Using this formula and the related parameters in the age Equations (45) and (46) yields the results reported in Table 2 (the corresponding SC results are also shown in this table).

As it can be seen from the values in this table, the KCC age of the Universe is, in both cases, in agreement with the accepted estimates. In KCC, there is also no apparent age problem for the Quasar APM 08279+5255: our first estimate (1.65 Gyr) is greater than the lowest age limit of 1.5 Gyr , while our second estimate (2.45 Gyr) is larger than the best estimated age for this quasar of 2.1 Gyr .

5. Conclusions

In this work we analyzed KCC in view of recent astrophysical data from SNIa and determinations of the Hubble parameter as a function of redshift. The analysis of the supernova data essentially confirmed our previous work on the subject, but this time we used the recent Union 2.1 data (580 data points, instead of 292) and more general assumptions for our KCC fitting formulas.

It was shown that the KCC model can again accommodate all existing SNIa data, without resorting to dark energy, or to any other exotic component of the Universe. Moreover, the current value of the Hubble constant was derived directly from the SNIa data, using the KCC model, without any prior assumption for this value. We obtained a KCC estimate of the Hubble constant as $\mathbf{H}_0 = 67.53 \text{ km s}^{-1} \text{ Mpc}^{-1}$, very

close to the 2013 Planck collaboration value. The other KCC fundamental parameters, δ , γ , κ , and k , were critically re-evaluated and their updated values reported in Equation (36).

KCC was also tested against OHD for $H(z)$ and in relation with the age of the Universe and of old quasars. As in the case of luminosity distance determinations, it was found that age determinations in KCC need to be corrected by using the same scale factors which are at the basis of our model. With these scale corrections, KCC can effectively accommodate the existing $H(z)$ data, and does not show any apparent age problem, including the case of quasar APM 08279+5255.

Therefore, our final conclusion is that kinematical conformal cosmology is still a viable alternative cosmological model, although surely not as popular as other models based on conformal gravity, or standard Λ CDM cosmology. Further studies will be needed to check this model against other astrophysical data in order to see if it remains a possible alternative cosmology.

Acknowledgments

The author would like to thank Loyola Marymount University and the Seaver College of Science and Engineering for continued support and for granting a sabbatical leave of absence to the author, during which this work was completed. The author is indebted to Z. Burstein for helpful comments and for proofreading the original manuscript. Finally, the author also thanks the anonymous referees for their valuable suggestions and useful comments, which helped improve the final version of this paper.

Conflicts of Interest

The author declares no conflict of interest.

References

1. Mannheim, P.D. Alternatives to dark matter and dark energy. *Prog. Part. Nucl. Phys.* **2006**, *56*, 340–445.
2. Clifton, T.; Ferreira, P.G.; Padilla, A.; Skordis, C. Modified Gravity and Cosmology. *Phys. Rept.* **2012**, *513*, 1–189.
3. Beringer, J.; Arguin, J.F.; Barnett, R.M.; Copic, K.; Dahl, O.; Groom, D.E.; Lin, C.J.; Lys, J.; Murayama, H.; Wohl, C.G.; *et al.* Review of Particle Physics (RPP). *Phys. Rev. D* **2012**, *86*, 010001.
4. Weyl, H. Reine Infinitesimalgeometrie. *Math Z.* **1918**, *2*, 384.
5. Mannheim, P.D.; Kazanas, D. Exact Vacuum Solution to Conformal Weyl Gravity and Galactic Rotation Curves. *Astrophys. J.* **1989**, *342*, 635–638.
6. Kazanas, D.; Mannheim, P.D. General Structure of the Gravitational Equations of Motion in Conformal Weyl Gravity. *Astrophys. J. Suppl.* **1991**, *76*, 431–453.
7. Mannheim, P.D. Linear potentials and galactic rotation curves. *Astrophys. J.* **1993**, *419*, 150–154.
8. Mannheim, P.D. Are galactic rotation curves really flat? *Astrophys. J.* **1997**, *479*, 659.
9. Mannheim, P.D.; O'Brien, J.G. Impact of a global quadratic potential on galactic rotation curves. *Phys. Rev. Lett.* **2011**, *106*, 121101.

10. Mannheim, P.D.; O'Brien, J.G. Fitting galactic rotation curves with conformal gravity and a global quadratic potential. *Phys. Rev. D* **2012**, *85*, 124020.
11. O'Brien, J.G.; Mannheim, P.D. Fitting dwarf galaxy rotation curves with conformal gravity. *Mon. Not. R. Astron. Soc.* **2012**, *421*, 1273–1282.
12. Mannheim, P.D.; O'Brien, J.G. Galactic rotation curves in conformal gravity. *J. Phys. Conf. Ser.* **2013**, *437*, 012002.
13. Mannheim, P.D. Cosmic Acceleration as the Solution to the Cosmological Constant Problem. *Astrophys. J.* **2001**, *561*, doi:10.1086/323206.
14. Varieschi, G.U. A Kinematical Approach to Conformal Cosmology. *Gen. Rel. Grav.* **2010**, *42*, 929–974.
15. Varieschi, G.U. Kinematical Conformal Cosmology: fundamental parameters from astrophysical observations. *ISRN Astron. Astrophys.* **2011**, *2011*, 806549.
16. Varieschi, G.U. Conformal Cosmology and the Pioneer Anomaly. *Phys. Res. Int.* **2012**, *2012*, 469095.
17. Varieschi, G.U. Kerr Metric, Geodesic Motion, and Flyby Anomaly in Fourth-Order Conformal Gravity. *Gen. Rel. Grav.* **2014**, *46*, 1741.
18. Diaferio, A.; Ostorero, L.; Cardone, V.F. Gamma-ray bursts as cosmological probes: LambdaCDM vs. conformal gravity. *JCAP* **2011**, *1110*, 008.
19. Yang, R.; Chen, B.; Zhao, H.; Li, J.; Liu, Y. Test of conformal gravity with astrophysical observations. *Phys. Lett. B* **2013**, *727*, 43–47.
20. Mannheim, P.D. Making the Case for Conformal Gravity. *Found. Phys.* **2012**, *42*, 388–420.
21. Bender, C.M.; Mannheim, P.D. No-Ghost Theorem for the Fourth-Order Derivative Pais-Uhlenbeck Oscillator Model. *Phys. Rev. Lett.* **2008**, *100*, 110402.
22. Bender, C.M.; Mannheim, P.D. Exactly solvable PT-symmetric Hamiltonian having no Hermitian counterpart. *Phys. Rev. D* **2008**, *78*, 025022.
23. Flanagan, É.É. Fourth order Weyl gravity. *Phys. Rev. D* **2006**, *74*, 023002.
24. Pireaux, S. Light deflection in Weyl gravity: critical distances for photon paths. *Classical Quant. Grav.* **2004**, *21*, 1897–1913.
25. Horne, K. X-ray gas in the galaxy cluster Abell 2029: conformal gravity versus dark matter. *Mon. Not. R. Astron. Soc.* **2006**, *369*, 1667–1676.
26. Diaferio, A.; Ostorero, L. X-ray clusters of galaxies in conformal gravity. *Mon. Not. R. Astron. Soc.* **2009**, *393*, 215–223.
27. Elizondo, D.; Yepes, G. Can conformal Weyl gravity be considered a viable cosmological theory? *Astrophys. J.* **1994**, *428*, 17–20.
28. Yoon, Y. Problems with Mannheim's conformal gravity program. *Phys. Rev. D* **2013**, *88*, 027504.
29. Riegert, R.J. Birkhoff's Theorem in Conformal Gravity. *Phys. Rev. Lett.* **1984**, *53*, 315–318.
30. Sultana, J.; Kazanas, D.; Said, J.L. Conformal Weyl gravity and perihelion precession. *Phys. Rev. D* **2012**, *86*, 084008.
31. Turyshv, S.G.; Toth, V.T. The Pioneer Anomaly. *Living Rev. Rel.* **2010**, *13*, 4; Available online: <http://www.livingreviews.org/lrr-2010-4> (accessed on 1 December 2014).

32. Turyshev, S.G.; Toth, V.T.; Kinsella, G.; Lee, S.C.; Lok, S.M.; Ellis, J. Support for the thermal origin of the Pioneer anomaly. *Phys. Rev. Lett.* **2012**, *108*, 241101.
33. Kowalski, M.; others. Improved Cosmological Constraints from New, Old and Combined Supernova Datasets. *Astrophys. J.* **2008**, *686*, 749–778.
34. Amanullah, R.; Lidman, C.; Rubin, D.; Aldering, G.; Astier, P.; Barbary, K.; Burns, M.S.; Conley, A.; Dawson, K.S.; Deustua, S.E.; *et al.* Spectra and Hubble Space Telescope Light Curves of Six Type Ia Supernovae at $0.511 < z < 1.12$ and the Union2 Compilation. *Astrophys. J.* **2010**, *716*, 712–738.
35. Suzuki, N.; Rubin, D.; Lidman, C.; Aldering, G.; Amanullah, R.; Barbary, K.; 1,2, Barrientos, L.F.; Botyanszki, J.; Brodwin, M.; Connolly, N.; *et al.* The Hubble Space Telescope Cluster Supernova Survey: V. Improving the Dark Energy Constraints Above $z > 1$ and Building an Early-Type-Hosted Supernova Sample. *Astrophys. J.* **2012**, *746*, 85.
36. Riess, A.G.; Macri, L.; Casertano, S.; Lampeitl, H.; Ferguson, H.C.; Filippenko, A.V.; Jha, S.W.; Li, W.; Chornock, R. A 3% Solution: Determination of the Hubble Constant with the Hubble Space Telescope and Wide Field Camera 3. *Astrophys. J.* **2011**, *730*, 119.
37. Ade, P.A.R.; Aghanim, N.; Armitage-Caplan, C.; Arnaud, M.; Ashdown, M.; Atrio-Barandela, F.; Aumont, J.; Baccigalupi, C.; Banday, A.J.; *et al.* Planck 2013 results. XVI. Cosmological parameters. *Astron. Astrophys.* **2014**, *571*, A16.
38. Moresco, M.; Cimatti, A.; Jimenez, R.; Pozzetti, L.; Zamorani, G.; Bolzonella, M.; Dunlop, J.; Lamareille, F.; Mignoli, M.; Pearce, H.; *et al.* Improved constraints on the expansion rate of the Universe up to $z \sim 1.1$ from the spectroscopic evolution of cosmic chronometers. *J. Cosmol. Astropart. Phys.* **2012**, *8*, 6.
39. Gaztañaga, E.; Cabré, A.; Hui, L. Clustering of luminous red galaxies - IV. Baryon acoustic peak in the line-of-sight direction and a direct measurement of $H(z)$. *Mon. Not. R. Astron. Soc.* **2009**, *399*, 1663–1680.
40. Jimenez, R.; Verde, L.; Treu, T.; Stern, D. Constraints on the Equation of State of Dark Energy and the Hubble Constant from Stellar Ages and the Cosmic Microwave Background. *Astrophys. J.* **2003**, *593*, 622–629.
41. Simon, J.; Verde, L.; Jimenez, R. Constraints on the redshift dependence of the dark energy potential. *Phys. Rev. D* **2005**, *71*, 123001.
42. Stern, D.; Jimenez, R.; Verde, L.; Kamionkowski, M.; Stanford, S.A. Cosmic chronometers: constraining the equation of state of dark energy. I: $H(z)$ measurements. *J. Cosmol. Astropart. Phys.* **2010**, *2*, 8.
43. Zhang, C.; Zhang, H.; Yuan, S.; Zhang, T.J.; Sun, Y.C. Four new observational $H(z)$ data from luminous red galaxies in the Sloan Digital Sky Survey data release seven. *Res. Astron. Astrophys.* **2014**, *14*, 1221–1233.
44. Blake, C.; Brough, S.; Colless, M.; Contreras, C.; Couch, W.; Croom, S.; Croton, D.; Davis, T.M.; Drinkwater, M.J.; Forster, K.; *et al.* The WiggleZ Dark Energy Survey: joint measurements of the expansion and growth history at $z < 1$. *Mon. Not. R. Astron. Soc.* **2012**, *425*, 405–414.

45. Chuang, C.H.; Wang, Y. Measurements of $H(z)$ and $D_A(z)$ from the Two-Dimensional Two-Point Correlation Function of Sloan Digital Sky Survey Luminous Red Galaxies. *Mon. Not. Roy. Astron. Soc.* **2012**, *426*, 226–236.
46. Jimenez, R.; Loeb, A. Constraining cosmological parameters based on relative galaxy ages. *Astrophys. J.* **2002**, *573*, 37–42.
47. Moresco, M.; Jimenez, R.; Cimatti, A.; Pozzetti, L. Constraining the expansion rate of the Universe using low-redshift ellipticals as cosmic chronometers. *JCAP* **2011**, *1103*, 045.
48. Weinberg, S. *Cosmology*; Oxford University Press: Oxford, UK, 2008.

© 2014 by the author; licensee MDPI, Basel, Switzerland. This article is an open access article distributed under the terms and conditions of the Creative Commons Attribution license (<http://creativecommons.org/licenses/by/4.0/>).